

# Dual optical responses of phenothiazine derivatives: near-IR chromophore and water-soluble fluorescent organic nanoparticles†

Sheng-Yuan Su,<sup>a</sup> Hsin-Hung Lin<sup>b</sup> and Cheng-Chung Chang<sup>\*b</sup>

Received 3rd May 2010, Accepted 11th July 2010

DOI: 10.1039/c0jm01303j

We have designed a conventional one-step organic coupling synthetic method to prepare a series of 10*H*-phenothiazine (PTZ) derivative fluorophores and investigated their optical behavior under alkaline conditions. The unexpected proton detachment at N-10 position (10*N-H*) of these PTZ derivatives provides switching between the visible fluorophore and near infrared (NIR) chromophore. Both anionic forms of compounds PTZ-NH and PTZ-OH exhibit strong red emission in alkali DMSO solutions, whereas only anionic PTZ-OH exhibits the near infrared absorption wavelength at 1010 nm. Moreover, the unexpected green fluorescence is observed due to the formation of fluorescent organic nanoparticles (FONs) when PTZ-OH is dissolved in alkaline aqueous conditions. These results indicate that these compounds have the potential for use in alkaline sensor applications, especially in aqueous solution.

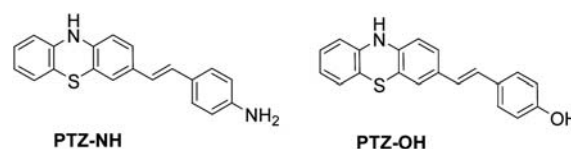
## Introduction

In recent years, fluorescent organic nanoparticles (FONs) have received considerable attention.<sup>1,2</sup> FONs differ from quantum dots and polymer nanoparticles in that they are expected to play various roles in a wide variety of applications such as optoelectronic devices due to the flexibility of the synthetic methods used in their production.<sup>2</sup> The switching of emission properties of FONs is often size-dependent and related to the effects of intramolecular planarization or specific intermolecular aggregation conformation. However, few studies have been conducted to date to evaluate the formation or application of FONs in pure aqueous solutions. On the other hand, there is currently a great deal of interest in near-infrared (NIR) absorbing dyes and pigments because of their potential applications in optoelectronic devices.<sup>3,4</sup> Specifically, NIR dyes play prominent roles in medicinal chemistry and biotechnology.<sup>5–7</sup> Functional dyes with significant bathochromic shifts are typically obtained by taking advantage of the strong donor–acceptor interactions that occur in these molecules<sup>8,9</sup> or by extending the  $\pi$ -system of the chromophores.<sup>10,11</sup> However, most of these dyes exhibit complex architectures that require multi-step synthetic procedures, which results in poor yields. In summary, it is possible to develop small organic molecules that provide dual photophysical properties: FONs and NIR chromophores for dual application.

The phenothiazine (PTZ) core has been considered to be an important moiety in heterocyclic chemistry since it was first reported in 1883.<sup>12</sup> Accordingly, PTZ is widely used in organic

light-emitting diodes (OLEDs),<sup>13,14</sup> acid–base dye pigments,<sup>15,16</sup> semiconductors,<sup>17–19</sup> and chemical sensors.<sup>20</sup> For particular examples, such as the methylene blue (MB) derivatives, the important pharmacological applications of PTZ are attributed to its stable radical cation heterocyclic form which can exhibit photodynamic therapy and near infrared fluorescence.<sup>21–23</sup> In this case, the proton 10*N-H* of PTZ is indispensable in the formation of stable radical cations but this leads to certain limitations for structural modifications. That is why there have been few reports of NIR chromophore from PTZ derivatives<sup>24–27</sup> and most of the above applications are based on the use of a protected PTZ structure with covalent substitutions on the nitrogen atom at the N-10-position (10*N-H*).

Recently, we described the convenient preparation of divinyl substituted 10*H*-phenothiazines at the 3- or 3, 7-positions without protecting group at the N-10 position and concluded that protonated PTZ derivatives can be used in cancer cell recognizer fluorophores due to their cation FONs behaviour.<sup>28</sup> Additionally, a detached proton from the 10*N-H* of PTZ derivatives can construct NIR ionic sensors dyes.<sup>29</sup> In the present study, a compound with dual photophysical properties was achieved under alkaline conditions; red emission in DMSO solution with NIR absorptive energy and green emission in aqueous solution due to the FONs formation. These optical phenomena were observed in PTZ-OH, but not in PTZ-NH (Scheme 1) or other control compounds. These findings indicate that the deprotonation of these PTZ derivatives on the nitrogen atom at the 10 position (10*N-H*) and the phenol parts are critically important and these fluorophores and NIR chromophores can eventually be switched on by the proton loss.



Scheme 1 The chemical structure of PTZ-NH and PTZ-OH.

<sup>a</sup>Department of chemistry, National Chung Hsing University 250, Kuo Kuang Road, Taichung 402, Taiwan, R.O.C.

<sup>b</sup>Graduate Institute of Biomedical Engineering, National Chung Hsing University 250, Kuo Kuang Road, Taichung 402, Taiwan, R.O.C. E-mail: ccchang555@dragon.nchu.edu.tw; Fax: +886-4-228 52422; Tel: +886-4-22840734 ext. 24

† Electronic supplementary information (ESI) available: Details of materials synthetic procedures, titration spectrum of PTZ-OH in Na<sub>3</sub>PO<sub>4</sub> (Fig. S1), FONs diagram of MPTZ-OH (Fig. S2). See DOI: 10.1039/c0jm01303j

## Synthesis and characterization of the PTZ fluorophores

**1. Materials.** The general chemicals employed in this study were of the best grade available and were obtained from Acros Organic Co., Merck Ltd, or Aldrich Chemical Co. and used without further purification. All solvents were of spectrometric grade. The starting materials 3-bromo-10*H*-phenothiazine (compound **1**) and 3-bromo-10-methyl-phenothiazine (compound **2**) were prepared according to the method described by Lin *et al.*<sup>29</sup>

**2. Apparatus.** Absorption spectra were generated using a *Thermo Genesis 6* UV-visible spectrophotometer, and fluorescence spectra were recorded using a *HORIBA JOBIN-YVON Fluoromas-4* spectrofluorometer with a 1 nm band-pass and a 1 cm cell length at room temperature. Transmission electron microscopy (TEM) was conducted on a *Zeiss EM 902A* operated at 80 kV. A solution of the PTZ derivatives (0.2 wt%) in deionized water was deposited onto a carbon-coated copper grid.

**3. Determination of quantum yields.** The quantum yields of PTZ derivatives were determined as previously described using the following equation:<sup>30</sup>

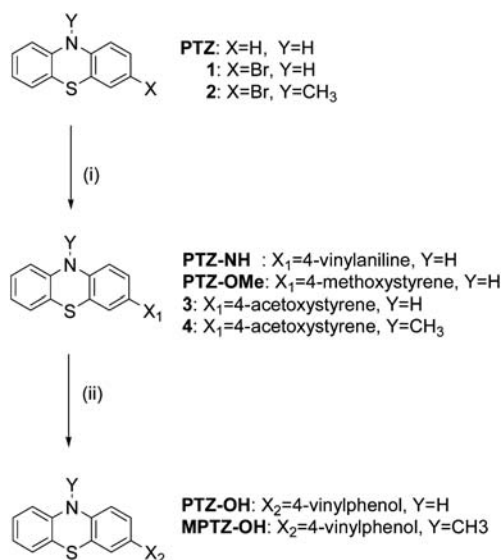
$$\Phi_u = \Phi_s \times [A_{fu} \times A_s(\lambda_{\text{exs}}) \times \eta_u^2] / [A_{fs} \times A_u(\lambda_{\text{exu}}) \times \eta_s^2]$$

where  $\Phi_u$  is the quantum yield of unknown;  $A_f$  is the integrated area under the corrected emission spectra;  $A(\lambda_{\text{ex}})$  is the absorbance area at the excitation wavelength;  $\eta$  is the refractive index of the solution; the subscripts u and s refer to the unknown and the standard, respectively. For the same  $\lambda_{\text{ex}}$ , we chose BMVC as the standard, which has a quantum yield of 0.25 in glycerol and 0.02 in DMSO.<sup>31</sup>

**4. General procedure for the synthesis of phenothiazine derivatives (Scheme 2).** Synthesis of the phenothiazine derivatives is shown in Scheme 1. 10*H*-phenothiazine or *N*-methyl-phenothiazine containing solutions were subjected to bromination with NBS/THF in an additional funnel. Next, the samples were subjected to the Heck coupling reaction<sup>32</sup> with 4-vinylaniline, 4-acetoxystyrene or 4-methoxystyrene using Pd(OAc)<sub>2</sub> as catalyst. Finally, 4-vinylphenol substituted PTZ derivatives were easily prepared by the addition of KOH in a methanol system.

### Molecular design and basic optical properties

3 Vinyl substituted PTZ derivatives were conveniently produced *via* a Heck reaction, their chemical structure and synthesis process are shown in Scheme 2. All products were in the *trans*-configuration as confirmed by the *J*-coupling constants of their spectra using nuclear magnetic resonance (NMR). In addition, their spectra presented well-defined extinction coefficients and high quantum yields in the visible region (Table 1). Reference compounds PTZ-OMe and MPTZ-OH were synthesized as a control for deprotonation of the phenol moieties and 10*N-H* of the PTZ derivatives, respectively. Furthermore, MPTZ-OH was used to examine the planarity of the PTZ core, which was absorbed at a higher energy (blue shift,  $\Delta\lambda \sim 10$  nm) than other PTZ derivatives. This was likely attributable to the presence of butterfly conformations caused by the steric effects of the



**Scheme 2** Synthesis of PTZ derivatives. Reaction reagents and conditions: (i) mixture of Pd(OAc)<sub>2</sub>/(*o*-tol)<sub>3</sub>P complex and 4-vinylaniline (for PTZ-NH) or 4-methoxystyrene (for PTZ-OMe) or 4-acetoxystyrene (for compound **3** and **4**) with Et<sub>3</sub>N/MeCN as a solvent pair. Reflux under nitrogen, 48 h. (ii) KOH, methanol, reflux, 4 h.

**Table 1** Basic spectral parameters of PTZ derivatives, NMR chemical shifts of 10*N-H*, extinction coefficients of absorption, and quantum yields of emission

	N-H <sup>a</sup>	O-H <sup>a</sup>	$\lambda_{\text{abs}}/\text{nm}$ ( $\epsilon \times 10^4$ ) <sup>b</sup>	$\lambda_{\text{em}}^c/\text{nm}$	$\Phi^d$
PTZ-NH	8.614	—	329 (2.67), 392 (2.43)	491	0.29
PTZ-OH	8.650	9.497	307 (3.14), 381 (1.61)	496	0.37
PTZ-OMe	8.664	—	307 (3.65), 380 (1.78)	505	0.46
MPTZ-OH	—	9.559	306 (2.77), 368 (1.84)	485	0.35

<sup>a</sup> Chemical shifts:  $\delta$  (ppm). <sup>b</sup> Absorption extinction coefficients: M<sup>-1</sup> cm<sup>-1</sup>. <sup>c</sup> Emission wavelength maximum excitation at the absorption maximum. <sup>d</sup> Fluorescence quantum yields.

substituents on the nitrogen atom at the 10 position as indicated by the folding angle.<sup>33</sup>

### Red fluorescence and NIR absorption from anionic PTZ

Fig. 1 shows the influence of deprotonation on the absorption and emission spectral shapes and  $\lambda_{\text{max}}$  of PTZ-NH. The  $\lambda_{\text{max}}$  values of the molecular absorptions showed marked bathochromic shifts when large excesses of bases ( $\sim 140$  equivalents (eq.)) were added to each of the dye solutions in DMSO. Uniform absorption peaks were produced at 550 nm with respect to the deprotonated PTZ-NH and red colour emission bands were observed at 620 nm in response to excitation at 550 nm. It should be noted that K<sub>2</sub>CO<sub>3</sub> presented a lesser degree of change in the absorption and emission spectra during the steady state, even when more than 500 equivalents of K<sub>2</sub>CO<sub>3</sub> were added. Thus, the ability of proton loss (10*N-H*) of PTZ-NH was estimated to be roughly comparable to that of K<sub>2</sub>CO<sub>3</sub>. In fact, emission peaks at 620 nm were also found with smaller quantum yield values when the samples were excited at 390 nm, which was

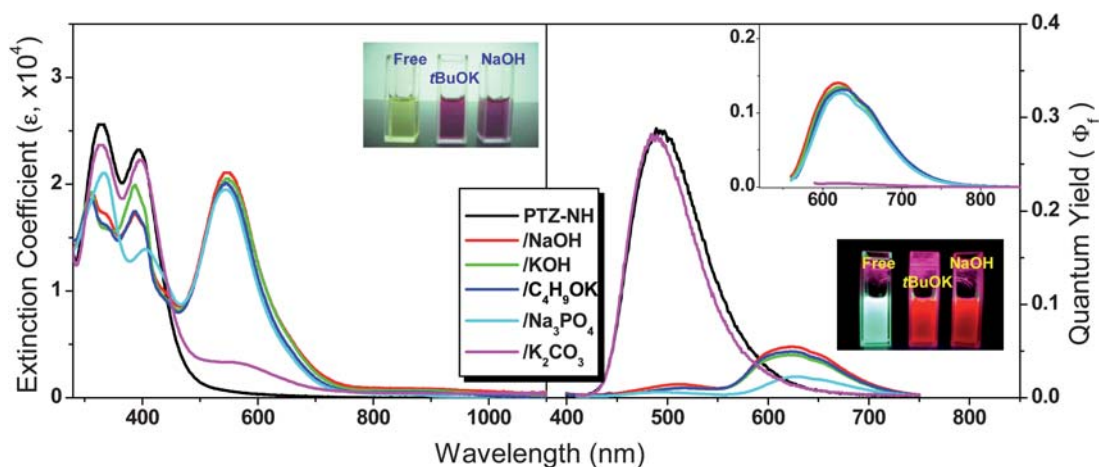


**Fig. 1** Absorption (left) and emission (right) spectra of PTZ-NH in alkaline DMSO solutions, represented by extinction coefficient and quantum yield, respectively. Excited wavelengths were 390 nm and 550 nm in the insert spectrum. The total concentrations of bases were 3.5 mM. Insert photos show the white light and visible emission images under UV light (365 nm).

ascribed to enhancement of the dissociation ability of 10N-*H* of PTZ in the excited state. However, the unexpected enhancement of dissociation of 10N-*H* of PTZ was due to extension of the  $\pi$ -system at the 3-positions of the PTZ derivatives.

Compound PTZ-OH showed more complicated deprotonation phenomena and spectral diversities than the other compounds (Fig. 2). The lowest absorption energy of deprotonated PTZ-OH could reach approximately 1010 nm in the near-IR region accompanied with the generation of 635 nm absorption bands in NaOH, KOH, *t*BuOK, and  $\text{Na}_3\text{PO}_4$ . It is interesting to note that the apparent 535 nm absorption bands were only observed in NaOH, KOH, and *t*BuOK; in the meantime, 600 nm emission bands were observed in response to excitation of deprotonated PTZ-OH at 535 and 420 nm. On the basis of the results of PTZ-NH, the peak at 535 nm should reflect the absorption of simple detachment of 10N-*H* of PTZ-OH, while the peaks at 635 and 1010 nm should be concerned with proton loss of the phenol portion of PTZ-OH. Note the spectrum

of control compound PTZ-OME in alkaline DMSO solution, as shown in Fig. 3. The spectral signals of deprotonated PTZ-OME were very similar to those of deprotonated PTZ-NH, with absorption at 545 nm and emission at 645 nm. The spectral diversities of these compounds as we mention above were because deprotonation of 10N-*H* on PTZ-NH, PTZ-OH or PTZ-OME becomes easier than for starting material phenothiazine (PTZ in Scheme 1). This inference appeared more convincing when the  $^1\text{H}$  NMR spectra in the  $\text{DMSO-d}_6$  solutions were investigated (Table 1). The protons of 10N-*H* on PTZ derivatives were deshielded and were further downfield (to higher ppm values) when compared to PTZ (8.564 ppm).

On the other hand, Fig. 3 also shows the consistent absorption shifts from 370 to 415 nm and emission quenching when another control compound MPTZ-OH was dissolved in alkaline DMSO; but there were no other NIR absorption peaks or red emission bands observed in this system. It is reasonable to consider both PTZ-NH and PTZ-OME to have just one proton detached from

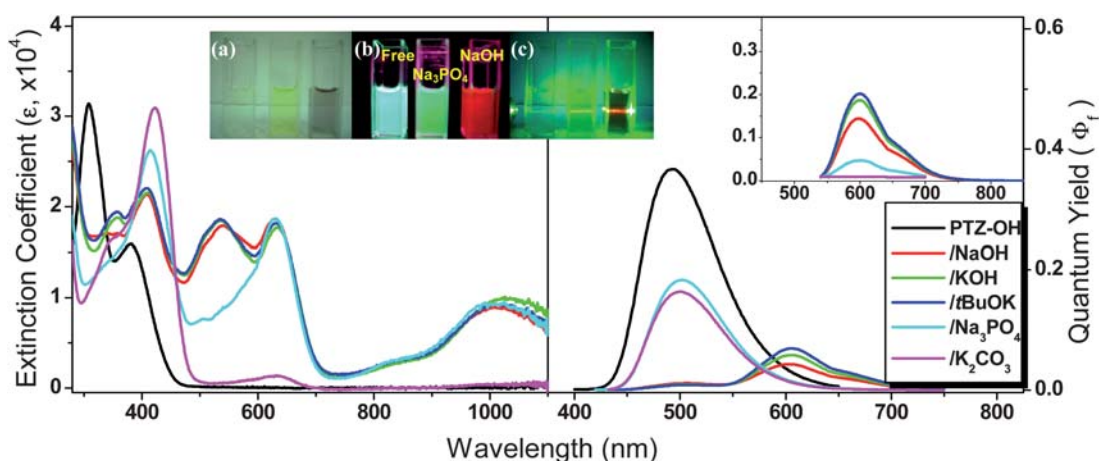


**Fig. 2** Absorption (left) and emission (right) spectra of PTZ-OH in alkaline DMSO solutions, represented by extinction coefficient and quantum yield, respectively. Excited wavelengths were 390 nm for free PTZ-OH and 410 nm for compounds in alkaline solution and 535 nm in the insert spectrum. The total concentrations of the bases were 3.5 mM. Insert photos show the white light (a), and the visible emission images under UV light (365 nm, b) and under 532 nm laser light (c).

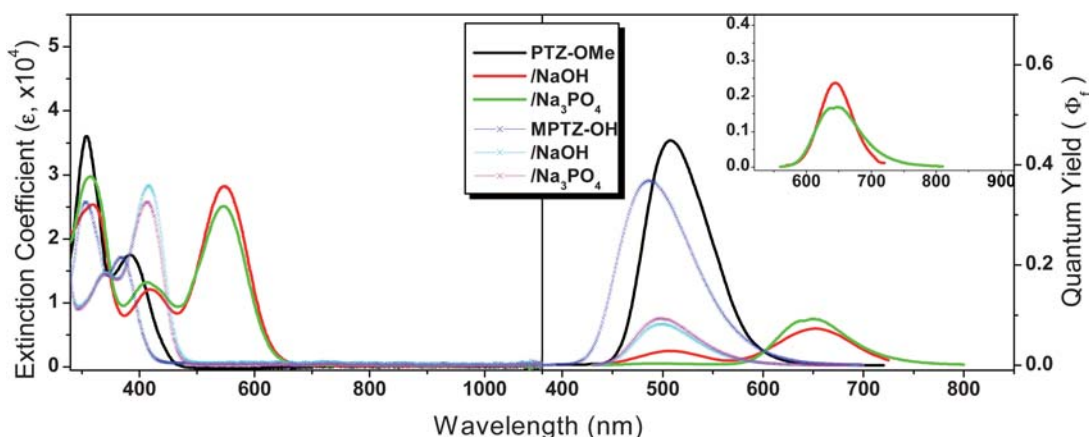
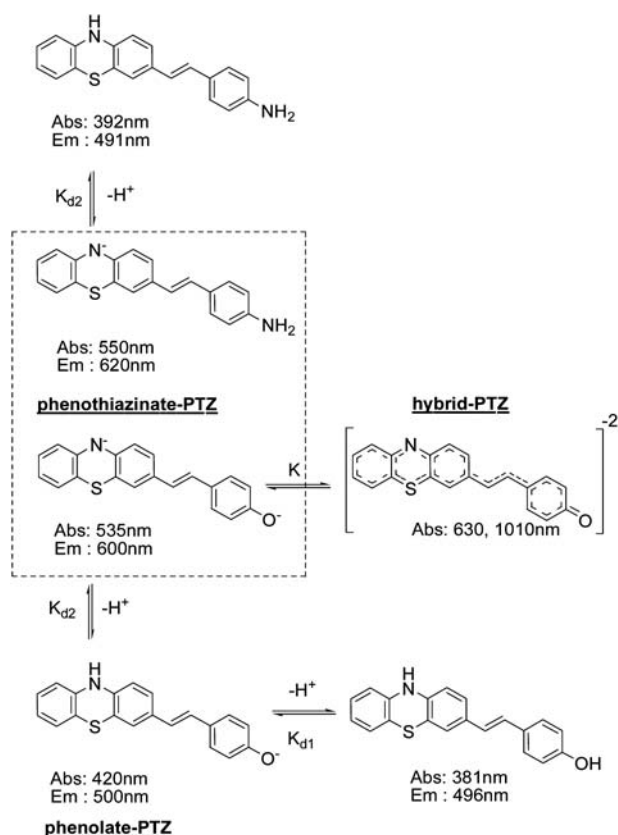


**Fig. 3** Absorption (left) and emission (right) spectra of PTZ-OMe and MPTZ-OH in alkaline DMSO solutions, represented by extinction coefficient and quantum yield, respectively. Excitation wavelengths were 390 nm for free compounds and 410 nm for compounds in alkaline solution and 550 nm in the insert spectrum. The total concentrations of the bases were 3.5 mM.



**Scheme 3** The possible deprotonation processes of PTZ-NH and PTZ-OH in alkaline DMSO solution.

the 10N-*H* of the phenothiazine part and then the phenothiazinate-PTZ anions were formed as in Scheme 3. These results infer that the individual characteristic absorption bands for phenolate-PTZ form (in Scheme 3) and the phenothiazinate-PTZ form of PTZ-OH should be observed at about 420 and 535 nm, respectively. And only phenothiazinate-PTZ can exhibit red fluorescence emission.

Fig. 4 shows the deprotonated titration spectrum of PTZ-OH in NaOH DMSO solution. Careful evaluation of the titration process revealed that deprotonation of the phenol moiety occurs in the first stage of titration, as indicated by the peak at 380 nm shifting to 420 nm with an isosbestic point at 342 nm. Then the peak at 540 nm grew due to loss of the proton of 10N-*H* with an isosbestic point at 465 nm during the second stage. Finally, the last process of the titration, the peak at 540 nm became flat and new bands appeared at 630 nm and 1010 nm simultaneously. The phenomenon of simultaneous peak growth was also observed during  $Na_3PO_4$  titration (Fig. S1†). We assumed that these two peaks were produced by either the electron delocalization between phenolate and phenothiazinate or hybridization of the sulfur atom.

Based on these results, the deprotonated processes for PTZ-OH in alkaline DMSO solution should be as proposed in Scheme 3. Since the trends in the spectral variations of deprotonated PTZ-OH were divided into two groups; with 535 nm absorption bands which exhibited red emission in NaOH, KOH,

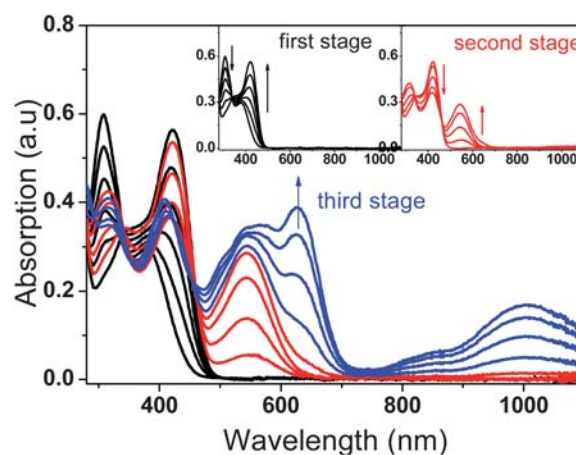


**Fig. 4** Deprotonated titration spectrum of PTZ-OH in NaOH-containing DMSO solution. Insert shows the first stage for the appearance of phenolate-PTZ and the second stage for the appearance of phenothiazinated PTZ.

and *t*BuOK and without 535 nm absorption bands in  $K_2CO_3$  and  $Na_3PO_4$ . These findings indicate that the observed phenomena are related to electron hybridization or delocalization between phenolate and phenothiazinate moieties of deprotonated PTZ-OH. Hence, ion exchange, contact ion-pair (CIP) or separated ion-pair (SIP) effects<sup>34–36</sup> should be taken into consideration mechanistically to explain the alkali-dependent spectra diversities. Once the CIP phenomenon exists in phenolate-PTZ or phenothiazinate-PTZ intermedium of Scheme 3, the generation probability of the hybrid-PTZ form should be decreased. The lifetime of phenothiazinate-PTZ may be long enough to observe red fluorescence.<sup>37,38</sup> There is no doubt that 10N-*H* of PTZ derivatives can be detached or partially detached by  $K_2CO_3$  and  $Na_3PO_4$ , however, their phenothiazinated-PTZ forms belong to the SIP form and are very transient in the excited state because their hybrid-PTZ forms develop very quickly. That is, the hybrid equilibrium *K* is more rapid than the second dissociation constant  $K_{d2}$  in the SIP system and the phenothiazinated-PTZ form can be rapidly converted into the hybrid-PTZ form. This explains why red emission can still be observed when a higher power 532 nm light source is applied (insert (c) of Fig. 2). Conversely, in the CIP system, the phenothiazinated-PTZ and hybrid-PTZ structures co-exist and stable red emission is observed at 600 nm in response to excitation at 535 nm.

#### Formation of FONs (fluorescent organic nanoparticles) and AIEE (aggregation-induced enhanced emission) effect in alkaline water

According to previous statements and discussions, the fluorescent intensities of deprotonated PTZ-OH should be decreased in the DMSO system, regardless of whether excitation occurred at 410 or 530 nm. Interestingly, fluorescence was dramatically enhanced when the PTZ-OH was dissolved in alkaline aqueous solution (as shown in Fig. 5). Contrary to the absorption spectra in DMSO (Fig. 2), the blue shifts of the lower energy peaks in the absorption spectra were assigned to H-aggregates of anionic PTZ-OH, which decrease the excited state thermal relaxation and lead to a dramatic increase in the fluorescence intensity. In previous studies, protonated PTZ derivatives were found to serve as surfactant-like molecules that further self-assemble to form

micelle-like nanoparticles due to their amphiphilic characteristics. And then, a FONs model was built in the case of water/aprotic solvent pair solutions.<sup>28</sup> In this case, the anionic PTZ-OH may also aggregate to form micelle-like nanoparticles (TEM images in Fig. 6) and an AIEE effect<sup>39</sup> was observed in alkaline aqueous solution with compound concentration from 1 to 100  $\mu$ M which did not need solvent pairs (shown in Fig. S3†). From the concentration-dependent fluorescence enhancement experiment, the AIEE effect achieved maxima when the concentration of anionic PTZ-OH was above 25  $\mu$ M; and eventually, the water-soluble FONs were developed.

Many reports have been published on specific counterion effects in micellar solutions of anionic or cationic surfactants. The addition of salt, depending on the system, can both destroy and induce a micellar structuring in solution.<sup>40,41</sup> In the course of this study we also investigated the FONs formation conditions of PTZ-OH in various alkaline aqueous solutions and in the presence of different concentrations of compounds. Fig. 6 shows the relationship between the emission intensity of anionic PTZ-OH and alkaline concentrations. The AIEE effects showed varying maximum quantum yields when the system was adjusted to

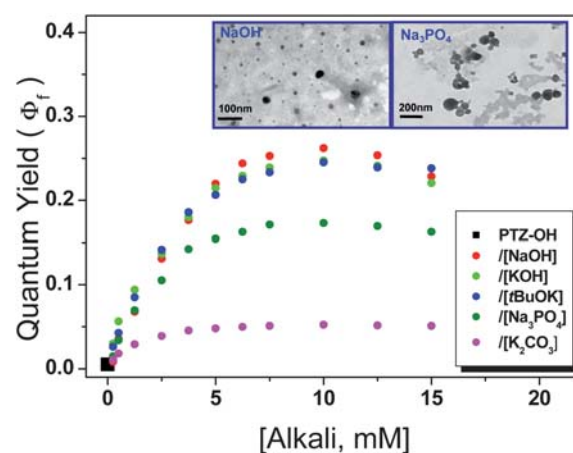


**Fig. 6** Alkali concentration dependent AIEE of PTZ-OH. Insets show the TEM images of nanoparticles obtained with the corresponding AIEE maxima solution.

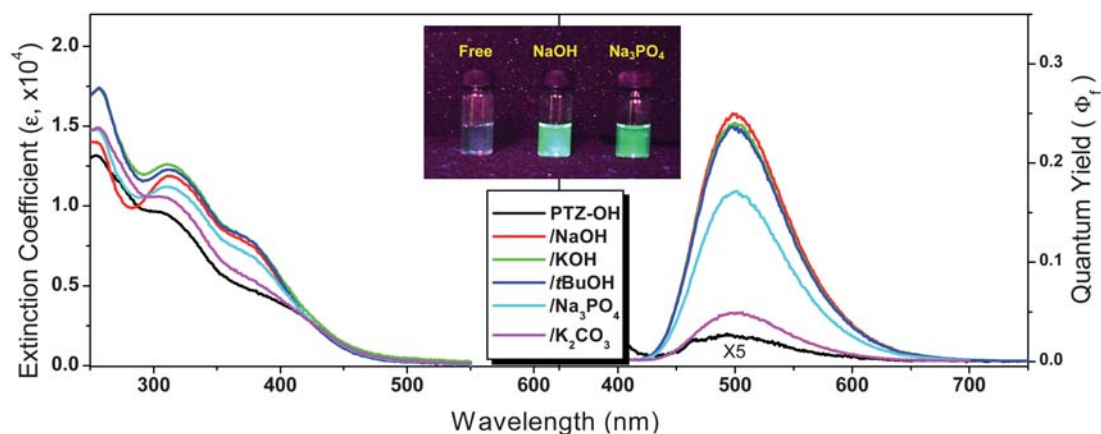


**Fig. 5** Absorption (left) and emission (right) spectral illustrations of 25  $\mu$ M PTZ-OH in alkaline aqueous solutions (10 mM). Insert photo shows the emission images under UV light (365 nm).

approximately 7.5 mM by the addition of alkali and the TEM images clearly showed that anionic PTZ-OH nanoparticles were spheres with mean diameters that ranged from 10 to 50 nm. It is noted that the quantum yields of Fig. 6 slightly decreased when an excess of base (more than 10 mM) was added to each of the dye solutions; this result once again confirmed the micelle construction theory in our case. Meanwhile, following the concentration-dependent AIEE result of Fig. S3,† the nanoparticles were also easily observed in TEM images of samples prepared using concentrations of PTZ-OH ranging from 5 to 100  $\mu$ M in alkaline aqueous solution. Furthermore, clear and intangible nanoparticle patterns were observed in NaOH and Na<sub>3</sub>PO<sub>4</sub> (insets of Fig. 6) systems, respectively, revealing the possibility of different counterion layers. This observation is concordant with the CIP or SIP theory described above. Similar results were observed for MPTZ-OH (Fig. S2†), indicating that deprotonation of phenol (phenolate-PTZ form in Scheme 3) is the dominant mechanism that leads to the formation of FONs, even though the phenothiazine-PTZ form is not apparent in the H<sub>2</sub>O system. Furthermore, neither PTZ-OH nor MPTZ-OH exhibited AIEE in neutral water solutions. Taken together, these findings indicate that the FONs model that was formed with aggregations of phenolate-PTZ, but not neutral PTZ derivatives or phenothiazine-PTZ. Thus, it is reasonable to build a FONs model based on our studies, especially in the case of alkaline water solutions.

## Conclusions

We describe a convenient method for the preparation of novel phenothiazine derivatives with special optical features under alkaline environment. Most of these PTZ derivatives products exhibit red emission fluorescence in alkaline DMSO solution when exciting their visible absorption wavelength. Furthermore, anionic PTZ-OH showed NIR absorptive energy in DMSO solution due to the formation of a hybrid form and green emission in aqueous solution due to the FONs construction, respectively. The significant wavelength shifts and large fluorescence enhancement of PTZ-OH were easily seen with the naked eye. Additionally, spectral switching between NIR absorption and visible region fluorophores could be achieved in phenothiazine *via* a mechanism of either the loss or retention of protons and this compound is potentially useful for alkaline sensor applications, especially in aqueous solution.

## Acknowledgements

This work was supported financially by the National Science Council (NSC 98-2113-M-005 -013-) of Taiwan.

## Notes and references

1 H. S. Nalwa, H. Kasai, S. Okada, H. Oikawa, H. Matsuda, A. Kakuta, A. Mukoh and H. Nakanishi, *Adv. Mater.*, 1993, **5**, 758; H. Kasai, H. Kamatani, Y. Yoshikawa, S. Okada, H. Oikawa, A. Watanabe, O. Itoh and H. Nakanishi, *Chem. Lett.*, 1997, 1181; H. B. Fu and J. N. Yao, *J. Am. Chem. Soc.*, 2001, **123**, 1434; B. K. An, S. K. Kwon and S. Y. Park, *Angew. Chem., Int. Ed.*, 2007, **46**, 1978.

2 J. Luo, Z. Xie, J. Y. Lam, L. Cheng, H. Chen, C. Qiu, H. S. Kwok, X. Zhan, Y. Liu, D. Zhu and B. Z. Tang, *Chem. Commun.*, 2001, 1740; B. K. An, S. K. Kwon, S. D. Jung and S. Y. Park, *J. Am. Chem. Soc.*, 2002, **124**, 14410; D. Xiao, L. Xi, W. Yang, H. Fu, Z. Shuai, Y. Fang and J. Yao, *J. Am. Chem. Soc.*, 2003, **125**, 6740; Y. Y. Sun, J. H. Liao, J. M. Fang, P. T. Chou, C. H. Shen, C. W. Hsu and L. C. Chen, *Org. Lett.*, 2006, **8**, 3713; S. S. Palayangoda, X. Cai, R. M. Adhikari and D. C. Neckers, *Org. Lett.*, 2008, **10**, 281.

3 J. Fabian, H. Nakazumi and M. Matsuoka, *Chem. Rev.*, 1992, **92**, 1197.

4 K. Y. Law, *Chem. Rev.*, 1993, **93**, 449–86.

5 U. Mahmood and R. Weissleder, *Mol. Cancer Ther.*, 2003, **2**, 489.

6 Z. Cheng, J. Levi, Z. Xiong, O. Gheysens, S. Keren, X. Chen and S. S. Gambhir, *Bioconjugate Chem.*, 2006, **17**, 662.

7 E. Sasaki, H. Kojima, H. Nishimatsu, Y. Urano, K. Kikuchi, Y. Hirata and T. Nagano, *J. Am. Chem. Soc.*, 2005, **127**, 3684.

8 C. Kohl, S. Becker and K. Müllen, *Chem. Commun.*, 2002, 2778.

9 H. Langhals, *Angew. Chem., Int. Ed.*, 2003, **42**, 4286.

10 A. Tsuda and A. Osuka, *Science*, 2001, **293**, 79.

11 Y. Avlasevich and K. Müllen, *Chem. Commun.*, 2006, 4440.

12 A. Bernthsen and B. Dent, *Chem. Ges.*, 1883, **16**, 2996.

13 G. W. Kim, M. J. Cho, Y. J. Yu, Z. H. Kim, J. I. Jin, D. Y. Kim and D. H. Choi, *Chem. Mater.*, 2007, **19**, 42.

14 N. S. Cho, J. H. Park, S. K. Lee, H. K. Shim, M. J. Park, D. H. Hwang and B. J. Jung, *Macromolecules*, 2006, **39**, 177.

15 C. O. Okafor, *Dyes Pigm.*, 1986, **7**, 249.

16 R. R. Gupta, *Phenothiazines and 1,4-Benzothiazines-Chemical and Biomedical Aspects*, Elsevier, Amsterdam, 1988, ch. 2.

17 B. N. Achar and M. A. Ashok, *Mater. Chem. Phys.*, 2008, **108**, 8.

18 S. Aftergut and G. P. Brown, *Nature*, 1962, **193**, 361.

19 A. Knorr and J. Daub, *Angew. Chem., Int. Ed. Engl.*, 1996, **34**, 2664.

20 M. Hauck, J. Schonhaber, A. J. Zuccherro, K. I. Hardcastle, T. J. J. Muller and U. H. F. Bunz, *J. Org. Chem.*, 2007, **72**, 6714.

21 W. J. Albery, A. W. Foulds, K. J. Hall, A. R. Hillman, R. G. Edgell and A. F. Orchard, *Nature*, 1979, **282**, 793.

22 A. Mattana, G. Biancu, L. Alberty, A. Accardo, G. Delogu, P. L. Fiori and P. Cappuccinelli, *Antimicrob. Agents Chemother.*, 2004, **48**, 4520.

23 C. Wagner and H. A. Wagenknecht, *Org. Biomol. Chem.*, 2008, **6**, 48.

24 M. J. Cho, J. Y. Kim, J. H. Kim, S. H. Lee, L. R. Dalton and D. H. Choi, *Bull. Korean Chem. Soc.*, 2005, **26**, 77.

25 A. T. Peters and N. J. Wang, *Dyes Pigm.*, 1995, **28**, 281.

26 H. Spreitzer and J. Daub, *Chem.-Eur. J.*, 1996, **2**, 1150.

27 T. Okamoto, M. Kuratsu, M. Kozaki, K. Hirotsu, A. Ichimura, T. Matsushita and K. Okada, *Org. Lett.*, 2004, **6**, 3493.

28 H. H. Lin, S. Y. Su and C. C. Chang, *Org. Biomol. Chem.*, 2009, **7**, 2036.

29 H. H. Lin and C. C. Chang, *Dyes Pigm.*, 2009, **83**, 14.

30 L. F. Vieira Ferreira and Silvia M. B. Costab, *J. Lumin.*, 1991, **48–49**, 395.

31 C. C. Chang, S. H. Kuo, C. C. Kang and T. C. Chang, *J. Lumin.*, 2006, **119–120**, 84.

32 C. C. Chang, K. J. Chen and L. J. Yu, *J. Org. Chem.*, 1999, **64**(15), 5603; C. C. Chang, Y. J. Wu and T.-C. Chang, *J. Chin. Chem. Soc.*, 2003, **50**, 185.

33 A. W. Franz, F. Rominger and T. J. J. Muller, *J. Org. Chem.*, 2008, **73**, 1795.

34 P. Vandereecken, J. P. Soumillion, M. V. D. Auweraer and F. C. D. Schryver, *Chem. Phys. Lett.*, 1987, **136**, 441.

35 J. P. Soumillion, P. Vandereecken, M. V. D. Auweraer, F. C. D. Schryver and A. Schanck, *J. Am. Chem. Soc.*, 1989, **111**, 2217.

36 G. Sciaini, E. Marceca and R. Ferra'ndez-Prini, *Phys. Chem. Chem. Phys.*, 2006, **8**, 4839.

37 N. Chattopadhyay, *Int. J. Mol. Sci.*, 2003, **4**, 460.

38 L. Piñero, X. Calderón, J. Rodríguez, I. Nieves, R. Arce, C. García and R. Oyola, *J. Photochem. Photobiol., A*, 2008, **198**(1), 85.

39 B. K. An, D. S. Lee, J. S. Lee, Y. S. Park, H. S. Song and S. Y. Park, *J. Am. Chem. Soc.*, 2004, **126**, 10232.

40 C. A. Bunton and G. Savelli, *Adv. Phys. Org. Chem.*, 1986, **22**, 213.

41 S. Kumar, S. L. David, V. K. Aswal, P. S. Goyal and Kabir-ud-Din, *Langmuir*, 1997, **13**, 6461.